XXXVI Ibero-Latin American Congress on Computational Methods in Engineering
CILAMCE
Rio de Janeiro, 22-25 Nov 2015

GLOBAL COMPARISON OF ORTHODONTIC MOVEMENT BETWEEN A SIMPLIFIED COMPUTATIONAL MODEL AND EXPERIMENTAL MEASUREMENTS OF A SWINE TOOTH

Sara de Godoy Bueno

Marco André Argenta

saracwb@hotmail.com

marco.argenta@gmail.com

Universidade Federal do Paraná (UFPR)

Av. Cel. Francisco H. dos Santos, Jardim das Américas. CEP: 81530-900, Curitiba/PR, Brasil.

Ana Paula Gebert de Oliveira Franco

Hypolito José Kalinowski

anapaula.gebert@gmail.com

hjkalin@utfpr.edu.br

Universidade Tecnológica Federal do Paraná (UTFPR)

Av. Sete de Setembro, 3165, Rebouças. CEP: 80230-901, Curitiba/PR, Brasil.

Abstract. *This article compares the orthodontic movement obtained by specific external loading conditions using computational models and an experimental test of an ex vivo swine tooth (premolar). A simplified three-dimensional computer model considering linear elastic material behavior working with isotropic properties is assumed with a geometry obtained by solid reconstruction based on the tomography of the tooth used in the experimental test, which are analyzed by Finite Element Method (FEM). The global displacements are obtained from vertical ideal loading conditions. Experimental tests are performed using the same loads. The displacements are measured from a fiber Bragg grating (FBG) sensory system. Vertical compressive forces are applied to the tooth and the comparison between the displacements is performed. The differences between the results are evaluated and discussed in order to clarify how close the linear elastic simplified model approaches to the physical behavior of the tested orthodontic movement.*

Keywords: *Orthodontic movement, Finite element method, Simplified computer model, Experimental tests.*

1 INTRODUCTION

The orthodontic movement occurs within the alveolar bone, which is remodeled when subjected to external loads (Kawarizadeh et al., 2003). Tissue reactions of the assembly composed from the tooth, periodontal ligament (PDL) and alveolar bone indicate histological changes that correspond to the space traversed by the moved teeth. The biomechanical response is due to the combination of the constitutive properties of organic, inorganic components and fluids present in the assembly (Lin et al., 2013).

Through experimental tests it is possible to get the force-displacement relationships and check differences in the PDL mechanical properties that exist in a tooth (Chiba et al. 1990). Elastic properties of the PDL is commonly determined from displacements results obtained from experimental observations (Yoshida et al., 2001). However, because of the complex geometry of the PDL, it can be said that no mechanical method suitable for determining the material properties as they depend on many factors, such as loading conditions and the region under consideration (Mandel et al. 1986). For this reason, several experimental studies have been done on the mechanical behavior of the tooth–PDL–alveolar bone assembly considering various boundary conditions, justifying, then, the different experimental tests present in the current literature.

Computational models have also been developed and compared to experimental results in order to better understand the orthodontic movement. The method used the most for numerical analyze is the Finite Element Method (FEM), which potential is validated as a clinical tool for simulating the orthodontic movement (Ammar et al., 2011).

From the literature about the PDL, it becomes clear that it does not have a linear behavior mainly due to the non-linear mechanical characteristics related to age, body region and applied load direction (Toms et al., 2002). Thus, studies accounting for the PDL nonlinear behavior were developed, focusing, for instance, on its morphology (Cattaneo et al., 2005) and on its anisotropy (Provatidis, 2000). Moreover, studies were done specifically to understand the PDL mechanical behavior (Field et al., 2009) and to confront linear and nonlinear models (Toms at al. 2003).

In addition to the various computational and experimental models developed for the alveolar bone, tooth and PDL material properties, studies about the conditions (Williams et al. 1984) and loading types (Rudolph et al., 2001) were important, as these also influence orthodontic movement.

Nevertheless, in the current literature there are still discrepancies between computational models developed to characterize the behavior of the tooth movement, justifying, then, the need to study the reasons for these differences (Fill et al., 2012). This paper, in order to collaborate with studies, develops a three-dimensional computer model for analyzing the global orthodontic movement, which the goal is to compare the displacements results obtained in numerical analysis with the experimental test. A linear elastic model will be used to approximately represent the physical behavior of the jaw orthodontic movement under vertical compression loads of 3N and 6N.

2 MATERIALS AND METHODS

2.1 Experimental tests

The experimental test was performed on an *ex vivo* premolar swine tooth donated by a company called Bizinelli, located in Curitiba/PR, Brazil. The lower jaw used at the test came from discarded material, so the experimental study does not need the release of the Ethics Committee in Orthodontic Research to be carried on.

An orthodontic bracket is attached on the swine inferior premolar tooth and a self-drilling locking screw NeoOrtho is inserted into the maxillary bone. A fiber Bragg grating (FBG) is glued with cyanoacrylate onto the bracket and elongated until reaching the screw. Afterwards the bracket is glued with cyanoacrylate to a screw head. The assembly scheme is shown in Figure 1.

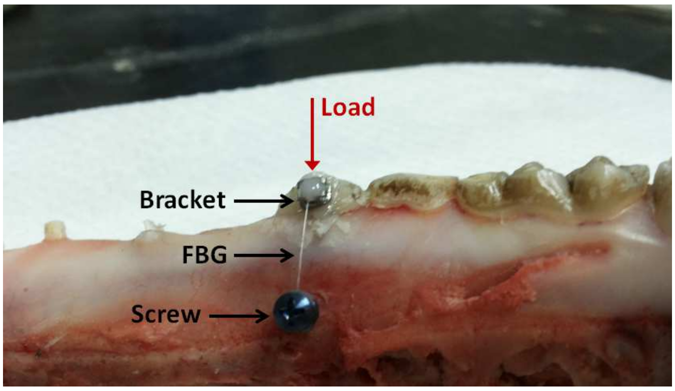

Figure 1. Assembly scheme for the sensorial test

Once the sensorial equipment has been assembled, the jawbone is placed on a test rig (EMIC DL100000) capable of applying localized compression forces of 3N and 6N on the tooth. The displacement measurements are recorded every 0.5s at a controlled velocity of 0.01 mm/s (Figure 2).


.

Figure 2. Assembly scheme for the compression test by EMIC

2.2 Computational model

For the finite element analysis an isotropic linear elastic material behavior was considered. The three-dimensional geometry was obtained via tomographic based solid reconstruction of the tooth used in the experimental test, yielding no significant differences between the computational model and the experimental jawbone. It was made about four hundred images via tomography. Three of them were shown in Figure 3, which shows a mesial, a occlusal and a buccal section view, respectively.

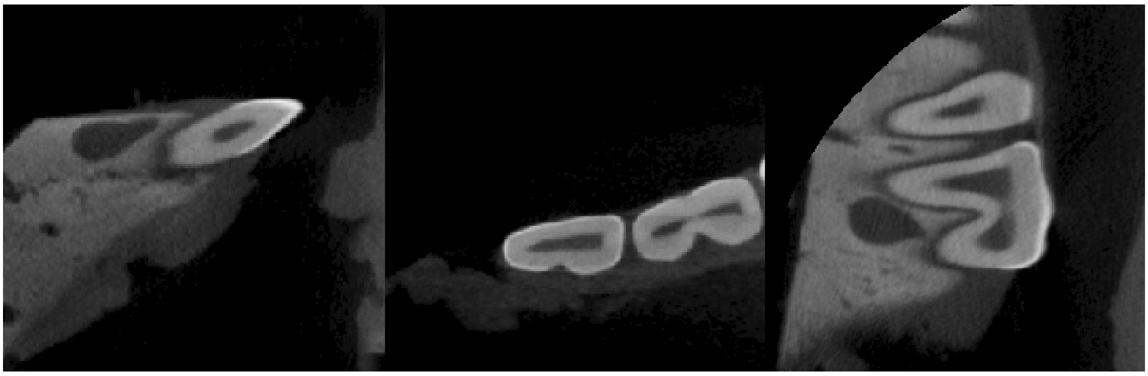

Figure 3. Tomography images from the swine tooth

The simplified three-dimensional computer model is composed of linear tetrahedral elements, as shown in Figure 4. A total of 97235 elements were used to mesh the alveolar bone, 45275 elements to mesh the dentine, 36754 elements to mesh the pulp, 19743 elements to mesh the enamel and 16433 to mesh the PDL.

The natural boundary conditions applied in the computational model are identical to the ones used in the experimental test, i.e., a vertical compressional load of 3N and subsequently 6N on the tooth.

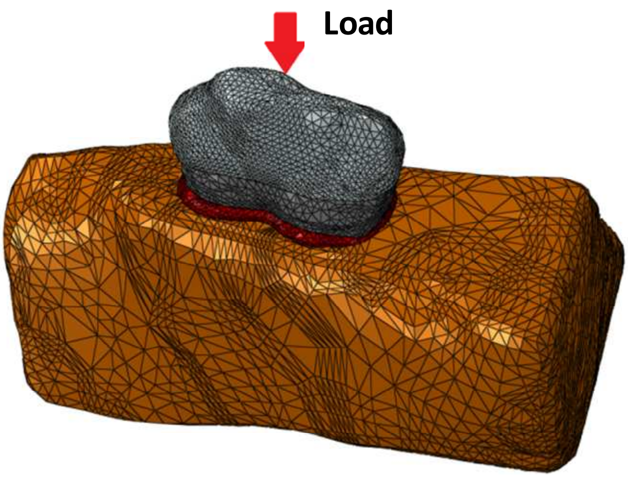

Figure 4. Linear tetrahedral finite element mesh

The Young's modulus (E) and the Poisson's ratio (υ) used for the alveolar bone (assuming homogeneous material), and the tooth PDL (this latter composed by enamel, dentin and pulp) were chosen based on data presented in current literature (Williams et al. 1984), shown in table 1.

Table 1. Structural material properties

Material	E (MPa)	υ
Dentin	18.600	0.30
Enamel	84.100	0.33
Pulp	2	0.45
Alveolar bone	13.800	0.30

The values of the Young's modulus and Poisson's ratio for the PDL were adjusted until the displacements obtained in the computational analysis were close enough to the obtained experimental displacements by EMIC.

3 RESULTS

3.1 Experimental tests

Forces and displacements are plotted from data generated by EMIC test rig for checking the mechanical behavior of the structure (Figures 5 and 6).

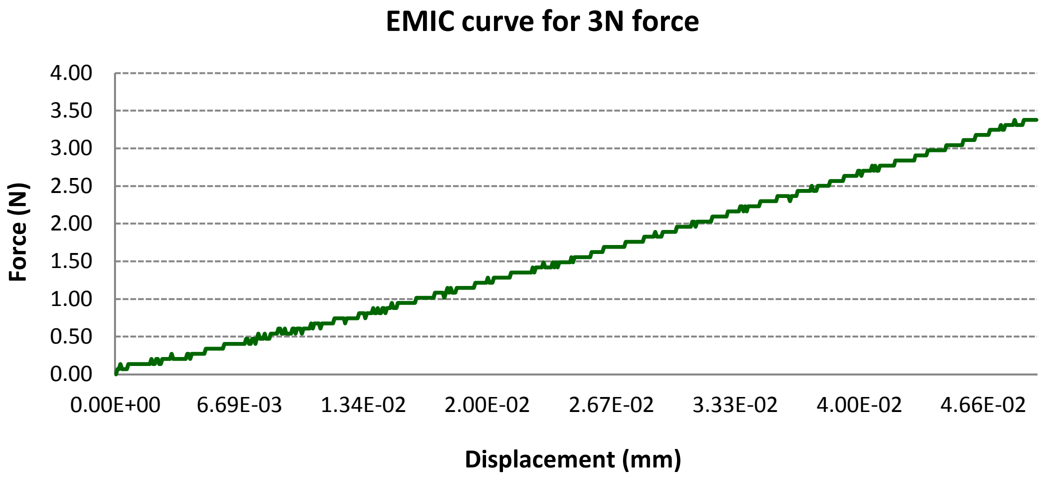

Figure 5. Relationship between force and displacement for force up to 3N

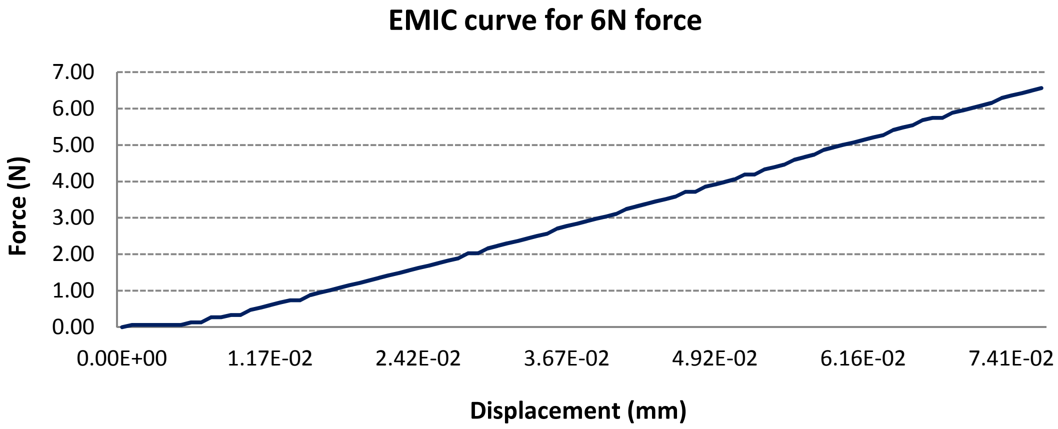

Figure 6. Relationship between force and displacement for force up to 6N

The global Young's modulus for characterizing the structure were calculated taking as reference the slope verified in each plotted curve, resulting in values of 70.82 MPa for 3N and 94.88 MPa for 6N.

The displacements obtained by the sensorial system are calculated from changes in the wavelength of Bragg grating, caused by longitudinal mechanical stresses due the photo-elastic effect inherent to the fiber. Figures 7 and 8 show the spectra for both loads, which gives the wavelength as a function of time. The first wavelength refers to the fiber positioned on the outer surface of the tooth, called buccal. The second wavelength refers to the fiber positioned on the inner face of the tooth, called tongue.

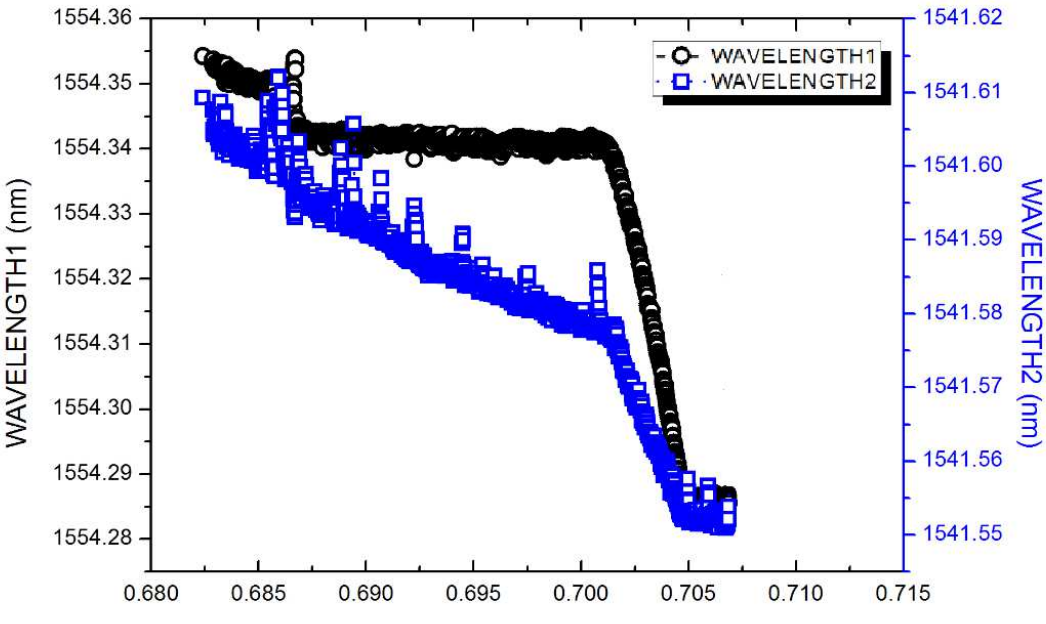

Figure 7. Spectral position of the Bragg grating for 3N force

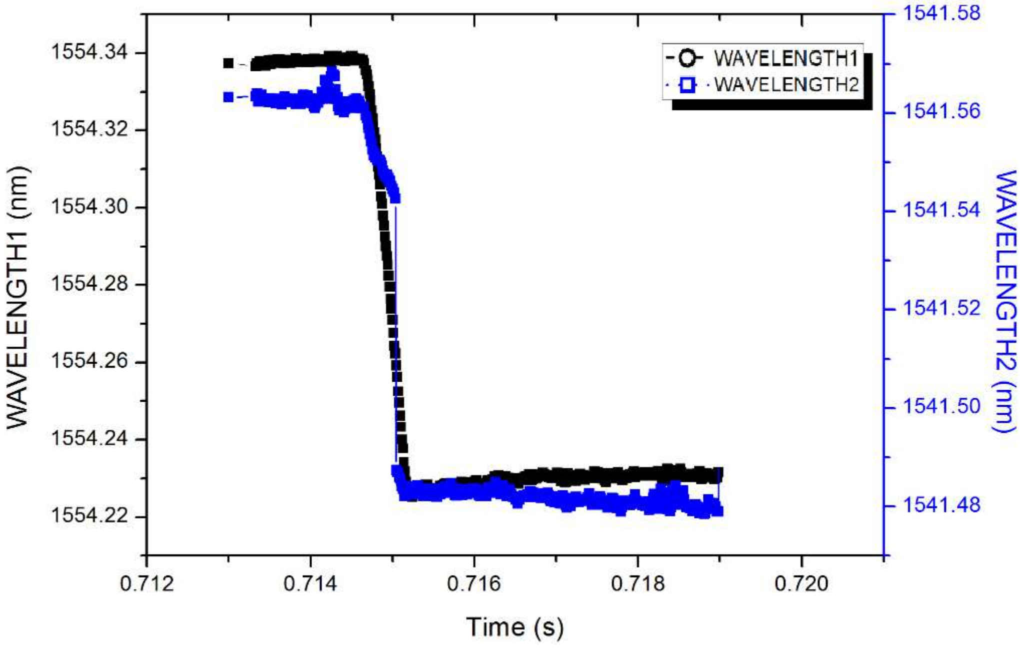

Figure 8. Spectral position of the Bragg grating for 6N force

The typical sensitivity of the optical sensor used in the experiment is $1.2\ \text{pm}/\mu\varepsilon$, that is, $1.2 \times 10^{-12}\text{m}/(\mu\text{m}/\text{m})$. Therefore, vertical displacements obtained for loads of 3N and 6N are, respectively, 0.0500mm and 0.0833mm.

3.2 Computational model

As noted above, the values of the Young's modulus and Poisson's ratio of the PDL were changed for each computer simulation performed until the displacements results were as close as possible to the experimental test. Once the desired displacement was obtained, the Young's modulus and Poisson's ratio were determined in the PDL, resulting in 0.24 MPa and 0.3, respectively.

The displacements results are shown in Figures 9 and 10, which present a longitudinal sectional model considering the deformed and undeformed configuration for each loading condition applied.

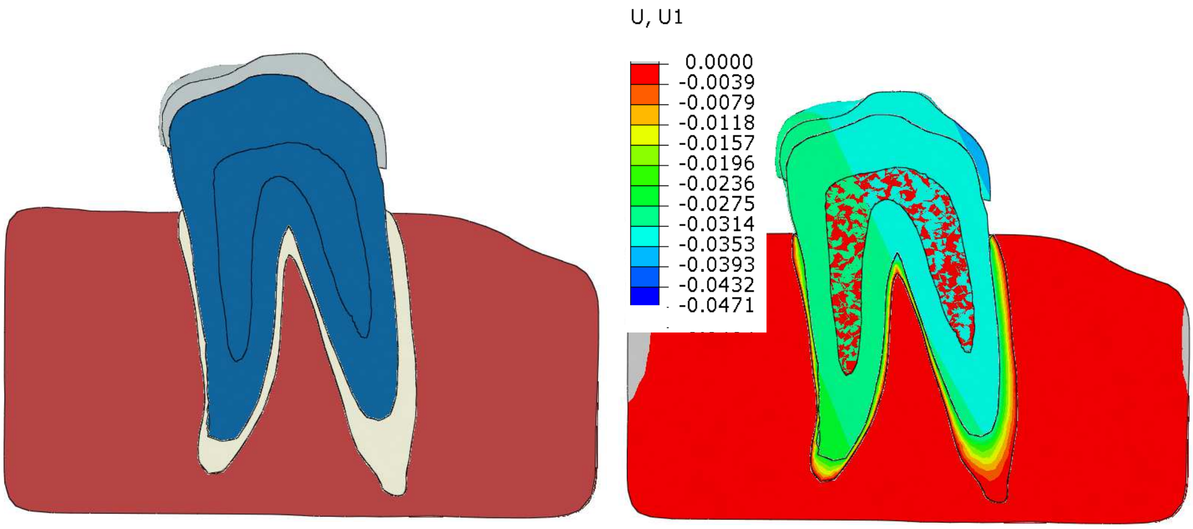

Figure 9. Longitudinal section for load of 3N

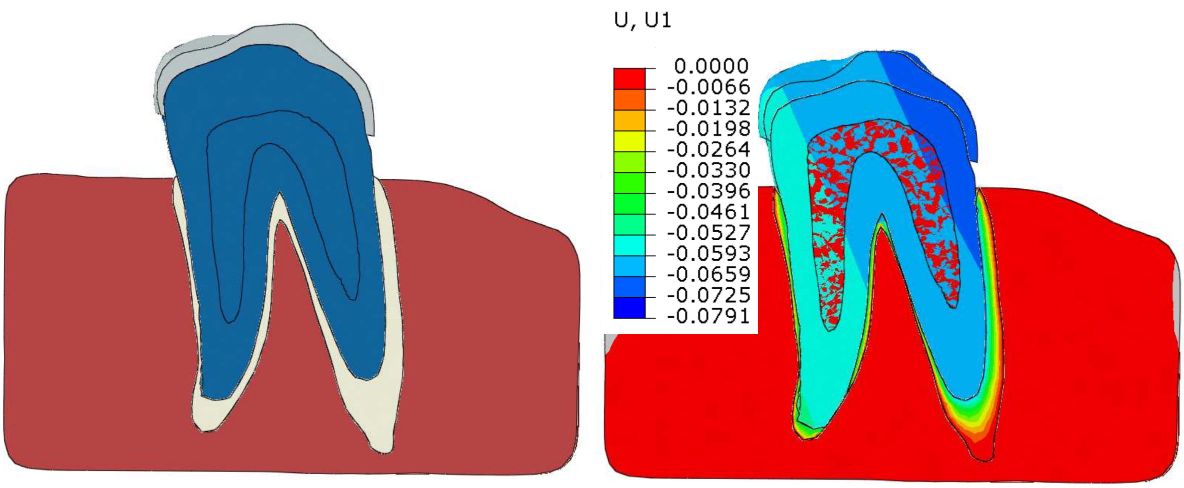

Figure 10. Longitudinal section for load of 6N

4 DISCUSSIONS

Previous studies showed several techniques for performing experimental testing and validated different computational models. Of which, a linear two-dimensional model was developed (Rees et al. 1997), a linear three-dimensional model (Jones, 2001) and (Panagiotopoulou at al., 2011), a three dimensional model incorporating the main fiber of the PDL (H. Qian et al., 2001), a nonlinear three-dimensional model (Kawarizadeh et al., 2003) and a contact model to represent the PDL without the need of a volumetric mesh (Tuna et al., 2014). Considerations about the type of work of PDL were also studied, considering hyperelastic model (Natali et al., 2004) and viscoelastic model (L. Qian et al., 2009) and (Wang et al., 2012).

This article presents a different technique for the experimental test using Bragg grating, which resulted in displacement values close to those obtained by the conventional experimental test, validating, thus, the methodology used.

Table 2 shows the results of maximum displacement obtained numerically and experimentally for each loading condition.

Table 2. Results of maximum displacements (mm)

Force (N)	Rede de Bragg test	EMIC test	Computational model
3	0.0500	0.0484	0.0419
6	0.0833	0.0785	0.0791

For 3N load, there is a variation of 3% between the maximum displacements results obtained by experimental tests. For 6N, the variation was double, 6%.

Comparing the displacements obtained by the test machine EMIC with the displacements of the computational model, a variation of 1% is verified to 3N load and 2.8% to 6N. This variation was small intentionally, since the model was adjusted so that the displacements were close, being the PDL Young's modulus the variable.

The curves relating forces to displacements in a synthesized manner are shown in Figure 11 to facilitate comparison between them.

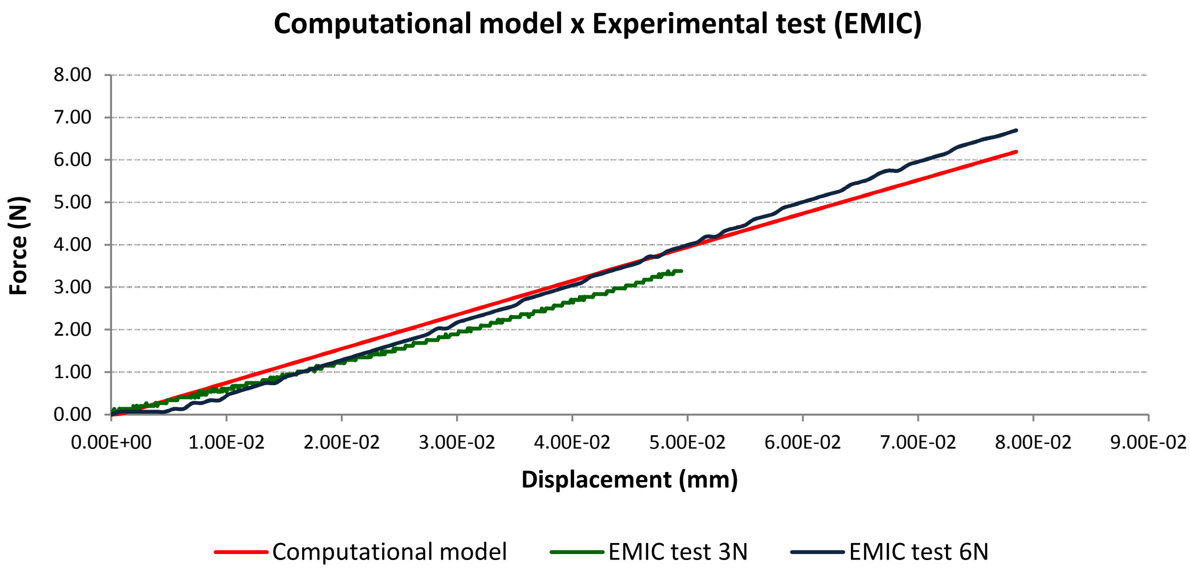

Figure 11. Comparison between curves of Force x Displacement

For the lower applied load, the curve is closer to a straight line than the higher one, it means, considering the Neumann's boundary conditions of this study, the simplified model to 3N load generates less error than to 6N load.

The global Young's modulus were calculated from the slope of each straight line, that were created doing an approximation of the curves obtained by experimental test. They are presented and compared in Table 3.

Table 3. Global Young's modulus

Force (N)	E (MPa) EMIC test	E (MPa) Computational model	Variation (%)
3N	70.82	78.91	11%
6N	94.88	78.91	20%

As expected, it is noted that the Young's modulus for the 3N load experimental model, when compared with the computational model, has a better numerical correlation than the 6N load experimental model.

5 CONCLUSIONS

The global displacements obtained experimentally and computationally were compared. The methodology for the experimental test using fiber Bragg grating demonstrated to be very effective in measuring the global displacements of the tooth movement. Furthermore, the experimental results correlate with those obtained via conventional compression tests conducted with the EMIC rig.

From the experimental testing, PDL and tooth assembly demonstrated a linear behavior and the proposed simplified computational model proved to be adequate. However, the Young's modulus does not provide an accurate parameter for the analysis models subjected to high intensity loads because the variation between the computational and experimental Young's modulus increases as the load increases.

Therefore, for the global analysis of orthodontic movement, the developed model has a satisfactory correlation with experimental results and can be used for loading conditions similar to those applied in this study, that is, low-intensity compression load. As this is a specific type of load, we cannot assume that the proposed model is valid for other loading conditions, such as shear, high intensity or tensile characteristics. For these specific cases, it is necessary to develop a model that best represents the real situation of the structure.

REFERENCES

Ammar, H. H., Ngan, P., Crout, R. J., Mucino, V. H., & Mukdadi, O. M., 2011. Three-dimensional modeling and finite element analysis in treatment planning for orthodontic tooth movement. *American Journal of Orthodontics and Dentofacial Orthopedics*, vol. 139, n. 1, pp. 59–71.

Cattaneo, P. M., Dalstra, M., & Melsen, B., 2005. The finite element method: a tool to study orthodontic tooth movement. *Journal of Dental Research*, vol. 84, n. 5, 428–433.

Chiba, M., Yamane, A., Ohshima, S., Komatsu, K., 1990. In Vitro Measurement of Regional Differences in the Mechanical Properties of the Periodontal Ligament in the Rat Mandibular Incisor. Archs. *Oral Biol.*, vol. 35, n. 2, pp. 153–161.

Field, C., Ichim, I., Swain, M. V., Chan, E., Darendeliler, M. A., Li, W., & Li, Q., 2009. Mechanical responses to orthodontic loading: A 3-dimensional finite element multi-tooth model. *American Journal of Orthodontics and Dentofacial Orthopedics*, vol. 135, n. 2, 174–181.

Fill, T. S., Toogood, R. W., Major, P. W., & Carey, J. P., 2012. Analytically determined mechanical properties of, and models for the periodontal ligament: Critical review of literature. *Journal of Biomechanics*, vol. 45, n. 1, pp. 9–16.

Jones, M. L., 2001. A Validated Finite Element Method Study of Orthodontic Tooth Movement in the Human Subject. *Journal of Orthodontics*, vol. 28, n. 1, pp. 29–38.

Kawarizadeh, a., Bourauel, C., & Jäger, a., 2003. Experimental and numerical determination of initial tooth mobility and material properties of the periodontal ligament in rat molar specimens. *European Journal of Orthodontics*, vol. 25, n. 6, pp. 569–578.

Lin, J. D., Özcoban, H., Greene, J. P., Jang, A. T., Djomehri, S. I., Fahey, K. P., Sunita, S. P., 2013. Biomechanics of a bone-periodontal ligament-tooth fibrous joint. *Journal of Biomechanics*, vol. 46, n. 3, pp. 443–449.

Mandel, U., Dalgaard, P., Viidik, A., 1986. A biomechanical study of the human periodontal ligament. *Journal of Biomechanics*, vol. 19, n. 8, pp. 637–645.

Natali, A. N., Pavan, P. G., & Scarpa, C., 2004. Numerical analysis of tooth mobility: Formulation of a non-linear constitutive law for the periodontal ligament. *Dental Materials*, vol. 20, n.7, pp. 623–629.

Panagiotopoulou, O., Kupczik, K., & Cobb, S. N., 2011. The mechanical function of the periodontal ligament in the macaque mandible: A validation and sensitivity study using finite element analysis. *Journal of Anatomy*, vol. 218, n. 1, pp. 75–86.

Provatidis, C. G., 2000. A comparative FEM-study of tooth mobility using isotropic and anisotropic models of the periodontal ligament. *Medical Engineering and Physics*, vol. 22, n. 5, pp. 359–370.

Qian, H., Chen, J., & Katona, T. R., 2001. The influence of PDL principal fibers in a 3-dimensional analysis of orthodontic tooth movement. *American Journal of Orthodontics and Dentofacial Orthopedics*, vol. 120, n. 3, pp. 272–279.

Qian, L., Todo, M., Morita, Y., Matsushita, Y., & Koyano, K., 2009. Deformation analysis of the periodontium considering the viscoelasticity of the periodontal ligament. *Dental Materials*, vol. 25, n. 10, pp. 1285–1292.

Rees, J. S., & Jacobsen, P. H., 1997. Elastic modulus of the periodontal ligament. *Biomaterials*, vol. 18, n. 14, pp. 995–999.

Rudolph, D. J., Willes PMG, & Sameshima, G. T., 2001. A finite element model of apical force distribution from orthodontic tooth movement. *The Angle Orthodontist*, vol. 71, n. 2, pp. 127–131.

Toms, S. R., & Eberhardt, A. W., 2003. A nonlinear finite element analysis of the periodontal ligament under orthodontic tooth loading. *American Journal of Orthodontics and Dentofacial Orthopedics*, vol. 123, n. 6, pp. 657–665.

Toms, S. R., Lemons, J. E., Bartolucci, A. a., & Eberhardt, A. W., 2002. Nonlinear stress-strain behavior of periodontal ligament under orthodontic loading. *American Journal of Orthodontics and Dentofacial Orthopedics*, vol. 122, n. 2, pp. 174–179.

Tuna, M., Sunbuloglu, E., & Bozdag, E., 2014. Finite element simulation of the behavior of the periodontal ligament: A validated nonlinear contact model. *Journal of Biomechanics*, vol. 47, n. 12, pp. 2883–2890.

Wang, C. Y., Su, M. Z., Chang, H. H., Chiang, Y. C., Tao, S. H., Cheng, J. H., Lin, C. P., 2012. Tension-compression viscoelastic behaviors of the periodontal ligament. *Journal of the Formosan Medical Association*, vol. 111, n. 9, pp. 471–481.

Williams, K. R., & Edmundson, J. T., 1984. Orthodontic tooth movement analysed by the Finite Element Method. *Biomaterials*, vol. 5, n. 6, pp. 347–351.

Yoshida, N., Koga, Y., Peng, C. L., Tanaka, E., & Kobayashi, K., 2001. In vivo measurement of the elastic modulus of the human periodontal ligament. *Medical Engineering & Physics*, vol. 23, n. 8, pp. 567–572.